

Synthesis and Structure–Activity Relationship for a Novel Class of Potent and Selective Carbamoyl-Triazole Based Inhibitors of Hormone Sensitive Lipase

Søren Ebdrup,* Lotte Gottlieb Sørensen, Ole Hvilsted Olsen, and Poul Jacobsen

Novo Nordisk A/S, Novo Nordisk Park, 2760 Måløv, Denmark

Received August 12, 2003

The central role of the intracellular enzyme hormone-sensitive lipase (HSL) in regulating fatty acid metabolism makes it an interesting pharmacological target for the treatment of insulin resistant and dyslipidemic disorders where a decrease in delivery of fatty acids to the circulation is desirable, e.g., in individuals with type 2 diabetes, metabolic syndrome, or impaired glucose tolerance. On the basis of a lead structure from high throughput screening, we have identified a very potent type of carbamoyl-triazole inhibitors of HSL. As part of the lead optimization program, four new classes of carbamoyl-triazoles were synthesized and tested with respect to potency, efficacy and selectivity. Methyl-phenyl-carbamoyl-triazoles were identified as potent and efficacious HSL inhibitors. These compounds do not inhibit other hydrolases such as hepatic lipase, lipoprotein lipase, pancreatic lipase, and butyrylcholine esterase. However, the inhibitors **4b** and **4g** with IC_{50} values for HSL of 0.17 and 0.25 μM , respectively, were the only inhibitors selective against acetylcholine esterase. A reversible pseudosubstrate inhibition mechanism is proposed for this class of inhibitors.

Introduction

Type 2 diabetes, including the metabolic syndrome, is a chronic multifactorial metabolic disease typically characterized by hyperinsulinemia, dyslipidemia, insulin resistance, and hyperglycemia. The disease is often associated with obesity, hypertension, and increased risk of cardiovascular disease.^{1,2} Due to the forecasted epidemic in type 2 diabetes,³ new therapies with few side effects and a robust effect and which address both the insulin resistance and dyslipidemic components of the disease are needed.^{3,4}

The elevated level of plasma fatty acids (FA) seen in type 2 diabetic patients is believed to be a major pathogenetic factor of the disease.^{5–7} The prevailing concept is that increased levels of FA as a result of increased net mobilization from adipose tissue in particular postprandially lead to peripheral insulin resistance,⁸ primarily via an inhibitory effect on muscle glucose uptake and usage.⁹ As a consequence, the blood glucose level will increase.¹⁰ Increased FA flux to the liver will also result in increased hepatic glucose output and an increased secretion of very low density lipoprotein elevating serum triglycerides (TG).¹¹ These events will contribute to the increased risk of cardiovascular disease seen in patients with type 2 diabetes and the metabolic syndrome.

The enzyme hormone-sensitive lipase (HSL), primarily expressed in adipose tissue, hydrolyses stored TG into monoglycerides and FA.¹¹ The enzyme is thought to be the rate-limiting enzyme in adipocyte lipolysis and net FA mobilization.¹² The monoglycerides are rapidly hydrolyzed by adipocyte monoacylglycerol lipase and thus do not accumulate.¹³

The activity of HSL is acutely regulated via a cAMP-protein kinase A mediated phosphorylation–dephos-

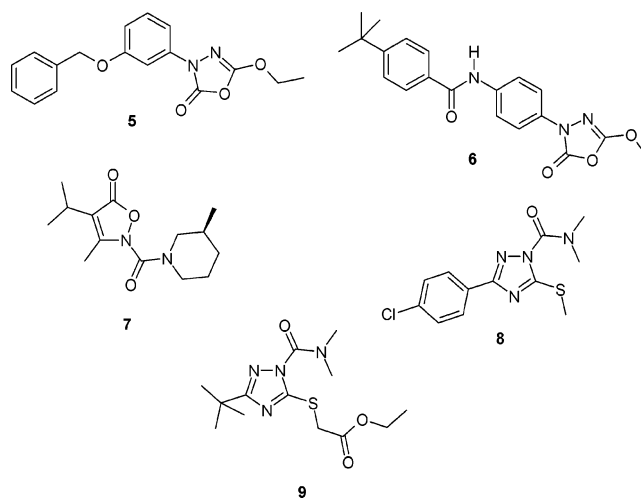


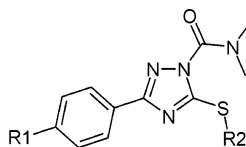
Figure 1. Chemical structure of related serine hydrolase inhibitors.

phorylation reaction.¹⁴ Adrenalin/noradrenalin and insulin indirectly stimulate or inhibit HSL, respectively.¹⁵ HSL is also regulated by alterations in the transcription of HSL.^{16,17}

In the fasted state, the levels of FA and glycerol in the circulation are primarily controlled by the lipolytic action of HSL on stored TG. Insulin resistance in adipocytes also enhances the net mobilization of FA by relieving the antilipolytic effect of insulin on HSL. The described central function of HSL in fat mobilization makes the enzyme a potential interesting pharmacological target for the treatment of disorders where a decrease in the level of FA in the circulation is desirable, such as in individuals with the metabolic syndrome and type 2 diabetes.

In this paper, a lead optimization program for a potent HSL inhibitor found in high throughput screening is presented together with counterscreening data for

* To whom correspondence may be addressed: fax, +45 44663939; phone, + 45 44434830; e-mail, sebd@novonordisk.com.

Table 1. Physical–Chemical Properties of Dimethyl Carbamoyl Triazoles

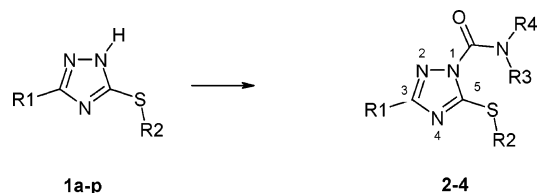
Compound No ^a	R1	R2	Mp/ °C	Recryst. Solvent	Molecular Formula ^b	Yield/ %
2a	Cl	Et	121.1	EtOAc	C ₁₃ H ₁₅ ClN ₄ OS, 1/5 mol % EtOAc	73
2b	Cl	Pr	94.5	EtOH	C ₁₅ H ₁₇ ClN ₄ OS	75
2c	Me	Me	134.8	Hept-MIK ^c	C ₁₃ H ₁₆ N ₄ OS	77
2d	Me	TfEt ^d	107.9	MeOH–H ₂ O	C ₁₄ H ₁₁ F ₃ N ₄ OS	70
2e	Me	Hex	33.0	EtOH–H ₂ O	C ₁₈ H ₂₆ N ₄ OS	61
2f	OTfMe ^e	Me	66.0	EtOH–H ₂ O	C ₁₃ H ₁₃ F ₃ N ₄ O ₂ S, 1/3 mol % EtOH	69
2g	OMe	Me	89.2	MeOH–H ₂ O	C ₁₃ H ₁₆ N ₄ O ₂ S	56
2h	TfMe ^f	Me	110.2	MeOH–H ₂ O	C ₁₆ H ₁₆ N ₄ OS	47
2i	Ph	Me	144.4	EtOH	C ₁₈ H ₁₈ N ₄ OS	80
2j			105.8	EtOH–H ₂ O	C ₁₆ H ₁₆ N ₄ OS	50
2k			130.2	MeOH	C ₁₄ H ₁₆ N ₄ OS	53

^a Carbamoyl chloride: dimethylcarbamoyl chloride. ^b C, H, N within $\pm 0.4\%$. ^c MIK: methyl isopropyl ketone. ^d TfMe: 1,1,1-trifluoroethyl. ^e Trifluoromethoxy. ^f Trifluoromethyl.

a selection of lipases and esterases. The selectivity and activity profiles for the most potent and selective HSL inhibitors identified are compared with three HSL inhibitors described by Aventis^{18,19} and Bayer.²⁰ In addition, a mechanism of inhibition for this novel type of HSL inhibitors will be proposed and compared with the expected inhibition mechanism for the HSL inhibitors described by Aventis and Bayer.

Chemistry

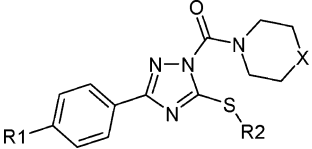
Different 3-phenyl- or 3-alkyl-5-alkylsulfanyl-4*H*-[1,2,4]triazoles (**1a–p**) were carbamoylated with different carbamoyl chlorides in DMF applying 1,4-diazabicyclo[2.2.2]octane (DABCO) as a base to give the respective carbamoylated-triazoles (**2–4**) (Figure 2, Tables 2–4, and general procedure 1). Since potentially three different isomeric *N*-carbamoylated triazoles can be formed, the position of carbamoylation was established by X-ray diffraction of crystals of compound **2h**. It was found that it is the N(1) isomer (Figure 2, corresponding to N(2), Figure 3) which is formed by the carbamoylation

**Figure 2.** Synthetic route to carbamoyl triazoles **2–4**.

protocol. Since compounds **2–4** are close analogues of **2h**, it is expected that all intermediates (**1a–p**) are carbamoylated at the same position.

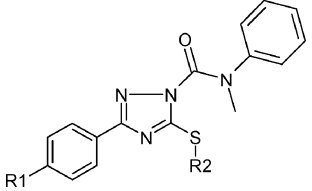
Results and Discussion

Despite a lack of amino acid sequence homology the 84-kDa HSL protein exhibits a remarkable secondary structure homology with a superfamily of esterases and lipases including acetylcholineesterase (AChE) and several fungal lipases.²¹ HSL belongs to a class of lipases and esterases that adopts the so-called α/β -hydrolase fold, and the active site is comprised of a catalytic triad and an oxyanion hole.

Table 2. Physical–Chemical Properties of Piperidine and Morpholine Triazole Carbamates


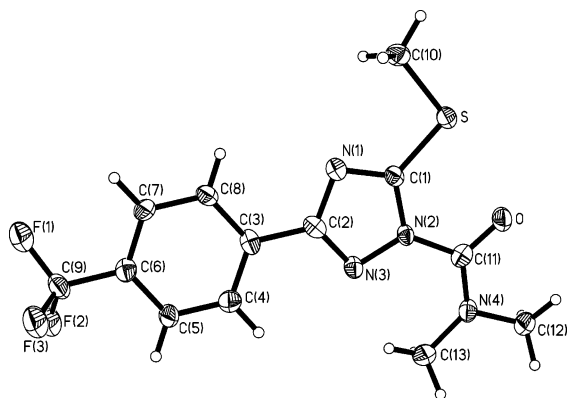
compd no.	R1	R2	X	mp/°C	recryst solvent	molecular formula ^a	yield/%
3a^b	Cl	Me	O ^c	128.8	MeOH	C ₁₄ H ₁₅ ClN ₄ O ₂ S	84
3b^b	Cl	TfEt ^d	O ^c	123.9	MeOH	C ₁₅ H ₁₄ ClF ₃ N ₄ OS	78
3c^e	Cl	Hex	O ^c	64.7	MeOH	C ₁₉ H ₂₅ ClN ₄ OS	81
3d	Me	Me	O ^c	110.3	EtOH	C ₁₃ H ₁₆ N ₄ O ₂ S	63
3e	OMe	Et	O ^c	98.1	MeOH–H ₂ O	C ₁₆ H ₂₀ N ₄ O ₃ S	68
3f	Cl	Me	CH ₂ ^f	101.7	MeOH	C ₁₅ H ₁₇ ClN ₄ OS	97
3g^b	Cl	TfEt ^c	CH ₂ ^f	115.3	MeOH	C ₁₆ H ₁₆ ClF ₃ N ₄ OS	84
3h	Cl	MeCy ^g	CH ₂ ^f	114.5	MeOH	C ₁₈ H ₂₁ ClN ₄ OS	56
3i^e	Cl	Hex	CH ₂ ^f	54.8	– ^h	C ₂₀ H ₂₇ ClN ₄ OS	82

^a C, H, N within ±0.4%. ^b Silica gel column chromatography, ethyl acetate/heptane 1:6 → 1:5). ^c Carbamol chloride: 4-morpholinylcarbonyl chloride. ^d TfEt: 1,1,1-trifluoroethyl. ^e Silica gel column chromatography, ethyl acetate/heptane 1:10 → 1:5). ^f Carbamol chloride: 1-piperidinecarbonyl chloride. ^g MeCy: methylcyclopropyl. ^h Colorless oil.

Table 3. Physical–Chemical Properties of Methyl Phenyl Carbamates


compd no. ^a	R1	R2	mp/°C	recryst solvent	molecular formula ^b	yield/%
4a	Cl	Me	99.8	MeOH	C ₁₇ H ₁₅ ClN ₄ OS	97
4b^c	Cl	TfEt ^d	101.9	MeOH	C ₁₈ H ₁₄ ClF ₃ N ₄ OS	80
4c	Cl	MeCy ^e	102.4	MeOH	C ₂₀ H ₁₉ ClN ₄ OS	76
4d^f	Cl	Hex	55.5	MeOH	C ₂₂ H ₂₅ ClN ₄ OS	89
4e	Me	Me	74.1	MeOH–H ₂ O	C ₁₈ H ₁₈ N ₄ OS	37
4f	Me	Hex	62.9	EtOH–H ₂ O	C ₂₃ H ₂₈ N ₄ OS ^g	50
4g^h	OTfMe	Me	97.1	MeOH–H ₂ O	C ₁₈ H ₁₅ F ₃ N ₄ O ₂ S	63
4h	OMe	Et	79.2	MeOH–H ₂ O	C ₁₉ H ₂₀ N ₄ O ₂ S	61

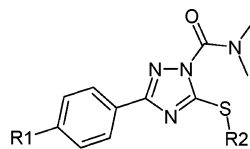
^a Carbamol chloride: *N*-methyl-*N*-phenylcarbonyl chloride. ^b C, H, N within ±0.4%. ^c Silica gel column chromatography, ethyl acetate/heptane 1:6 → 1:5). ^d TfEt: 1,1,1 trifluoroethyl. ^e MeCy: methylcyclopropyl. ^f Silica gel column chromatography, ethyl acetate/heptane 1:10 → 1:5). ^g H, N within ±0.4%, C: calcd, 67.62; found, 68.22. ^h Silica gel column chromatography, ethyl acetate/heptane (1:8).

**Figure 3.** ORTEP⁴³ drawing of **2h** with thermal ellipsoids shown at the 50% probability level.

HSL has a broad substrate specificity as it catalyses the hydrolysis of acylglycerols, cholesterol esters, lipoidal esters of steroid hormones, and retinyl esters while it has no or weak activity against phospholipids.^{22–25} Recently, interest in finding HSL inhibitors has increased, Aventis has filed patent applications on a class of potent oxadiazolones (**5**, **6**),^{18,19} and Bayer has published work on the potent HSL inhibitor 4-isopropyl-3-methyl-2-[1-(3-(*S*)-methylpiperidine-1-yl)-methanoyl]-2*H*-isoxazol-5-one (BAY) (**7**).²⁰

Optimization of HSL Inhibitors. A high throughput screening was performed to identify potent HSL inhibitors. Compound **8** was identified as a new and potent HSL inhibitor with an IC₅₀ value of 7 nM. The lead compound did not inhibit hepatic, lipoprotein, and pancreatic lipase using a triacylglycerol substrate. In contrast, potent inhibition of both butyrylcholine (BChE) and acetylcholine (AChE) esterase with IC₅₀ values < 100 nM was seen (Table 4). This was expected since the close analogue triazamate **9**²⁶ is a commercially available AChE-inhibiting insecticide.

A medicinal chemistry optimization program based on the lead structure **8** was initiated to find potent and more selective HSL inhibitors. Different R2 groups were combined with different R1 groups (Table 4). However, none of these compounds (**2a–2e**) showed any increased selectivity. Different R1 groups were also introduced for R2 being a methyl group (Table 4), but it was not possible to find a more potent or selective combination than the one seen for the lead compound **8**. The three analogues **2c**, **2f**, and **2h** were nevertheless potent HSL inhibitors with IC₅₀ values of 0.03, 0.1, and 0.1 μM, respectively. In general, a range of different substituents are tolerated at the R1 and R2 positions. None of the compounds shown in Table 4 were inhibitors of hepatic

Table 4. Activity and Selectivity of Dimethyl Carbamoyl Triazoles

Compound No	R1	R2	HSL IC ₅₀ (μ M)	Counter screen	
				AChE IC ₅₀ (μ M)	BChE IC ₅₀ (μ M)
8	Cl	Me	0.02	< 0.01	0.1
2a	Cl	Et	0.21 ± 0.11 ^d	0.05	0.056 ± 0.019 ^d
2b	Cl	Pr	0.06	0.1	0.3
2c	Me	Me	0.03	0.2	0.8
2d	Me	TfEt ^a	0.6	0.46 ± 0.19 ^d	0.2
2e	Me	Hex	> 50	0.3	0.2
2f	OTfMe ^b	Me	0.1	0.2 ± 0.12 ^d	0.8
2g	OMe	Me	0.9	0.41 ± 0.27 ^d	0.8
2h	TfMe ^c	Me	0.1	0.1	0.5
2i	Ph	Me	1.5 ± 0.54 ^d	0.23 ± 0.04 ^d	0.56 ± 0.27 ^d
2j			2	0.13 ± 0.073 ^d	0.050 ± 0.011 ^d
2k			> 50	0.37 ± 0.096 ^d	< 0.01

^a TFET: 1,1,1-trifluoroethyl. ^b OTfMe: trifluoromethoxy. ^c TfMe: trifluoromethyl. ^d Results are expressed as mean ± SEM, *n* = 2.

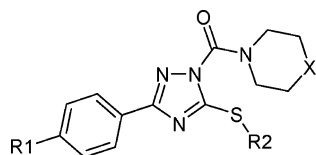
lipase (HL), lipoprotein lipase (LPL), and pancreatic lipase (PL) when tested in doses up to 50 μ M.

As it appeared to be difficult to find selective *N,N*-dimethyl carbamoyl-triazole based-HSL inhibitors, we decided to focus on other classes of carbamoyl-triazoles. Different morpholine and piperidine analogues were synthesized and tested. The morpholine analogues **3a–3e** (Table 5) were weak HSL inhibitors with IC₅₀ in the μ M range. While none of the morpholine analogues were inhibitors of BChE, HL, LPL, and PL, inhibition of AChE in the μ M range was seen making the compounds unselective. In contrast to this, the piperidine analogues (**3f**, **3g**, and **3h**, Table 5) were potent HSL inhibitors, e.g., **3f** was found to inhibit HSL with an IC₅₀ value of 0.1 μ M. Unfortunately, the piperidine analogues were not selective as they were also potent inhibitors of BChE

(0.026–0.3 μ M range) and weak inhibitors of AChE. None of the piperidine analogues were inhibitors of HL, LPL, and PL.

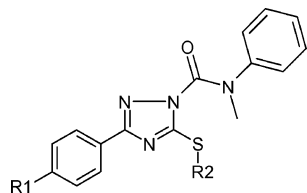
To examine whether increased steric hindrance close to the carbonyl group could be important for the selectivity profile, a range of *N*-methyl, *N*-phenyl carbamoyl-triazoles were synthesized. These compounds were potent HSL inhibitors with IC₅₀ values in the nM range (0.062–0.7 μ M) (Table 6). None of the HSL inhibitors showed any BChE, HL, LPL, or PL inhibition, but some were AChE inhibitors (**4a**, **4c**, **4e**, and **4h**).

The two compounds **4b** and **4g** did not inhibit any of the counterscreened enzymes and they were therefore identified as potent and selective inhibitors of HSL with IC₅₀ values of 0.17 and 0.25 μ M, respectively.

Table 5. Activity and Selectivity of Morpholine and Piperidine Carbamoyl Triazoles

compd no.	R1	R2	X	counterscreen		
				HSL IC ₅₀ (μM)	AChE IC ₅₀ (μM)	BChE IC ₅₀ (μM)
3a	Cl	Me	O	2	14 ± 9.2 ^c	>50
3b	Cl	TfEt ^a	O	9	>50	>50
3c	Cl	Hex	O	>50	>50	>50
3d	Me	Me	O	4	2	>50
3e	OMe	Et	O	9	4	>50
3f	Cl	Me	CH ₂	0.1	0.9	0.026 ± 0.007 ^c
3g	Cl	TfEt ^a	CH ₂	0.4	1	0.3
3h	Cl	MeCy ^b	CH ₂	0.2	0.9	0.1
3i	Cl	Hex	CH ₂	>50	>50	<0.01

^a TfEt: 1,1,1-trifluoroethyl. ^b MeCy: methylcyclopropyl. ^c Results are expressed as mean ± SEM, *n* = 2.

Table 6. Activity and Selectivity of *N*-Methyl-Phenyl Carbamoyl Triazoles

compd no.	R1	R2	HSL IC ₅₀ (μM)	AChE IC ₅₀ (μM)
4a	Cl	Me	0.16 ± 0.031 ^e	1.4 ± 0.01 ^e
4b	Cl	TfEt ^a	0.17 ± 0.11 ^e	>50
4c	Cl	MeCy ^b	0.062 ± 0.013 ^e	n.c. ^c
4d	Cl	Hex	0.4	>50
4e	Me	Me	0.1	2.4 ± 1.4 ^e
4f	Me	Hex	0.7	>50
4g	OTfMe ^d	Me	0.25 ± 0.005 ^e	>50
4h	OMe	Et	0.3	1.1 ± 0.18 ^e

^a TfEt: 1,1,1-trifluoroethyl. ^b MeCy: methylcyclopropyl. ^c n.c.: nonclassical inhibitor, with maximum HSL inhibition of 50%, *n* = 4. ^d OTfMe: trifluoromethoxy. ^e Results are expressed as mean ± SEM, *n* = 2.

The most potent and selective triazole based HSL inhibitors identified were compared with the three HSL inhibitors **5**, **6**, and **7**. Compounds **5** and **6** are among the most potent compounds described in each of two patent applications from Aventis,^{18,19} and **7** has been described by Bayer.²⁰ We have synthesized and analyzed these compounds for inhibition of HSL (Table 7) and found that compounds **6** and **7** inhibited HSL with IC₅₀ values of 0.023 and 0.17 μM, respectively, while compound **5** inhibited HSL with an IC₅₀ value of 1.1 μM. Compound **6** also inhibited HL (IC₅₀ = 1.8 μM) and LPL

Table 7. Comparison of the Activity and Selectivity of Selected HSL Inhibitors

compd no.	HSL IC ₅₀ (μM)	AChE IC ₅₀ (μM)	BChE IC ₅₀ (μM)	PL IC ₅₀ (μM)	LPL IC ₅₀ (μM)	HL IC ₅₀ (μM)
5	1.1 ± 0.073 ^a	0.92 ± 0.32 ^a	0.75	>10	>10	15 ± 7.2 ^a
6	0.023 ± 0.017 ^a	>50	>50	>10	0.20 ± 0.016 ^a	1.8 ± 0.42 ^a
7	0.17 ± 0.098 ^a	>50	17	>50	>50	>50
4b	0.17 ± 0.11 ^a	>50	>50	>50	>50	>50
4g	0.25 ± 0.005 ^a	>50	>50	>50	>50	>50

^a Results are expressed as mean ± SEM, *n* = 2.

(IC₅₀ = 0.20 μM), compromising its selectivity, while compound **7** was very selective with only weak inhibition of BChE (IC₅₀ = 17 μM). Compound **5** inhibits AChE and BChE with the same potency as inhibiting HSL and HL (IC₅₀ = 15 μM), making it unselective. In comparison **7** and the new carbamoyl-triazole based compounds **4b** and **4g** were all selective and potent inhibitors of HSL.

3D Model of HSL Active Site Based on Homology Modeling. Despite a low sequence homology to brefeldin A esterase²⁷ as well as to a thermophilic carboxylesterase,²⁸ which both have been solved by X-ray crystallography, the fold of the catalytic domain of HSL was nevertheless closely related to these structures. As mentioned above, this finding was first reported by Contreras et al.²¹ who constructed a three-dimensional model for the catalytic domain of HSL. On the basis of the sequence homology outlined,^{21,27} models of HSL have been built using the homology modeling program Modeller.²⁹ The large C-terminal portion and the major part of the regulatory domain of HSL are not included in the model. However, the active site (the catalytic triad (Ser424, His723 and Asp693)) and the oxy-anion hole (comprised of Gly353 and Ala425) and large parts of the substrate binding region are expected to be quite reliably modeled.^{21,30} As shown in Figure 4, the model is used to visualize the mechanism of action for the HSL inhibitor **4g**. Further, the model gave hints as to the presence of the regulatory domain which in the present model formed part of the substrate binding pocket. The modeled binding region has been used to describe the interaction to inhibitors, particularly in tetrahedral complex to the active site serine (Figure 4a). However, due to the low sequence homology and the lack of structural information about the regulatory domain, the predictive value of the model has been limited.

Proposed Mechanism of Inhibition. On the basis of the chemical structure, it is expected that all the HSL inhibitors **4b**, **4g**, **5**, **6**, and **7** are pseudosubstrates³¹ or pseudoirreversible inhibitors.³² It is believed that the inhibitors are capable of acylating the active site serine in a time-dependent manner as described for carbamates such as physostigmine³³ and postulated for oxadiazol-2-ones³⁴ (both AChE inhibitors). We postulate that the carbamoyl-triazole reacts with the HSL active site serine as described in Figures 4 and 5. The binding mode of **4g** over two steps along with the proposed reaction path is shown in Figure 4. Figure 4A depicts the tetrahedral complex covalently attached to the active site serine with the resulting oxy-anion stabilized by hydrogen bond interactions to the main chain nitrogens of Gly353 and Ala425. In Figure 4B the acyl complex is shown attached to the active site serine after

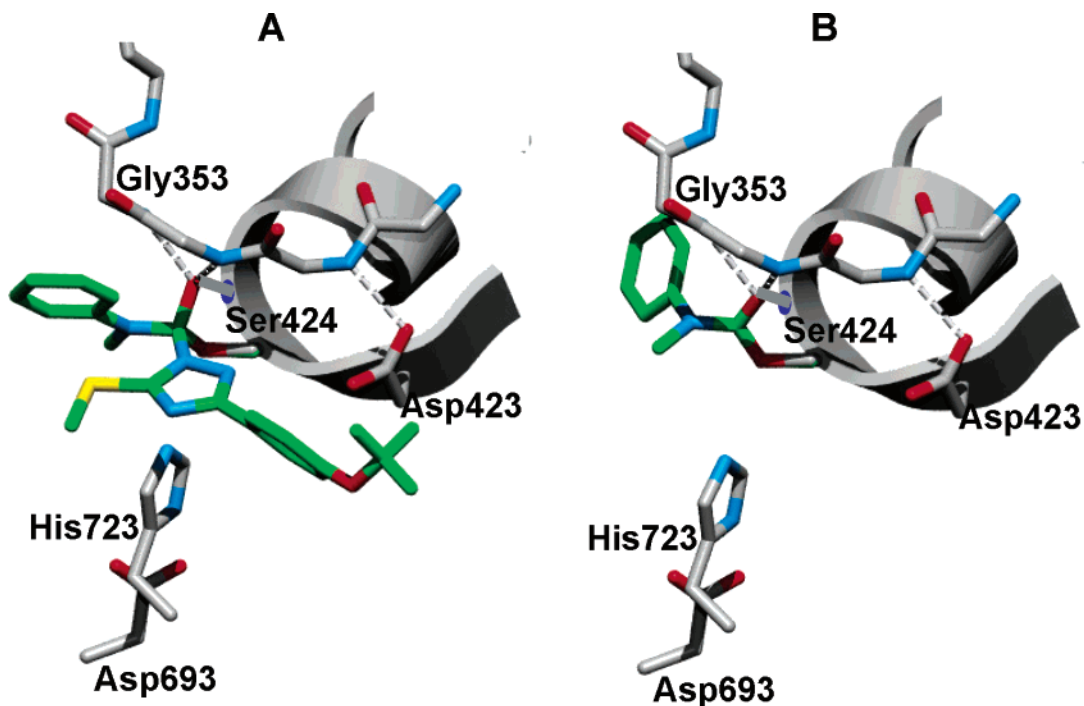


Figure 4. Models for the proposed reaction path for the inhibition of HSL by **4g**. In (A) the tetrahedral complex is shown while (B) shows the acylated active site HSL-serine.

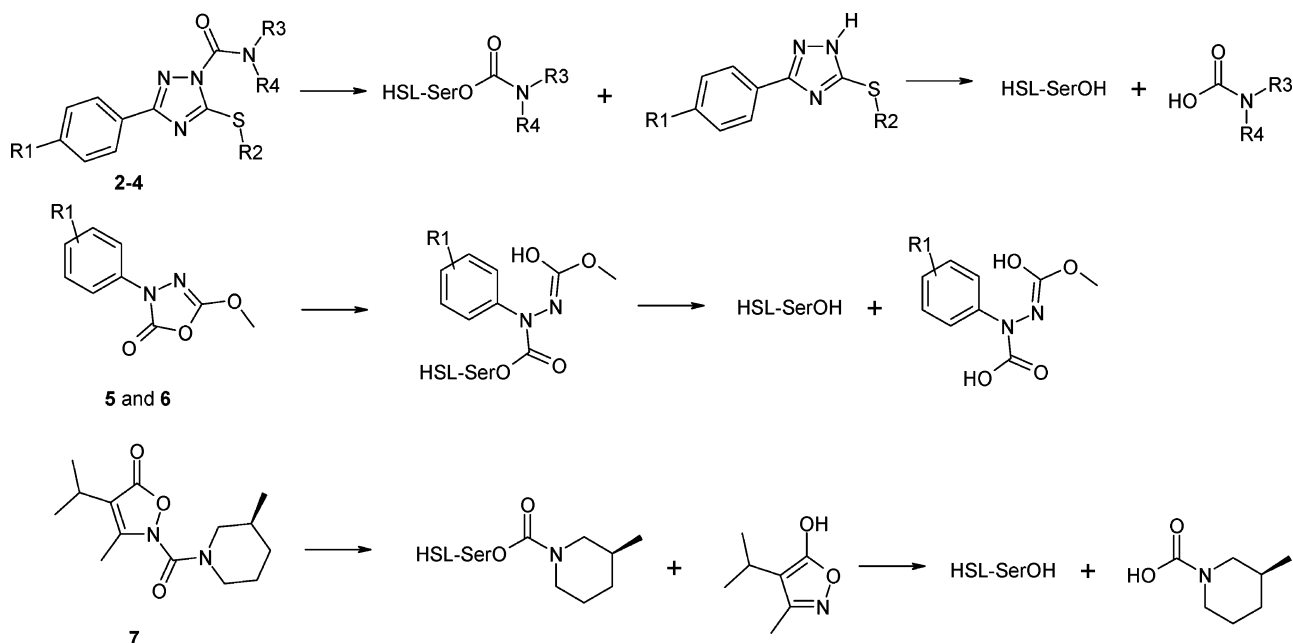


Figure 5. Hypothetical pseudosubstrate inhibition mechanism for HSL inhibitors.

cleavage of the triazole–carbonyl bond. In analogy with a phenol being the leaving group of carbamates, the triazole is expected to be the leaving group for the carbamoyl-triazoles.

The proposed inhibition mechanism for the carbamoyl-triazoles, **5**, **6**, and **7**, is shown in Figure 5. For both the carbamoyl-triazoles and compound **7** an analogous acylated HSL–serine intermediate is formed despite that different tetrahedral complexes are formed as the two types of compounds contain different leaving groups. Since the reactive groups of **5** and **6** are an isoxazole-5-one, the intermediate formed for this class of compounds is believed to be a ring open form as also suggested by Huang.³⁴

Preliminary studies of the reactivation rate of HSL for **4b** and **4g**, performed in accordance with the chromatographic method described by Perola et al.,³⁵ indicate that the reactivation half-life ($t_{1/2}$) is in the order of hours. This is in line with data for carbamate inhibitors of AChE.^{33,35,36} The reactivation rate of AChE is dependent on the size of the *N*-carbamate substituent as it is decreasing with increasing size,³⁶ indicating that *N*-methyl, *N*-phenyl carbamoyl-triazole (**4a–h**) inhibited HSL probably are reactivated with a slower rate than HSL inhibited with the smaller *N,N*-dimethyl carbamoyl-triazole analogues (**2a–k**). Further studies are needed to address the reactivation rate in vitro and in vivo, which is outside the scope of this paper.

Conclusion

We have identified a novel type of potent carbamoyl-triazole based inhibitors of hormone-sensitive lipase (HSL). It is expected that the compounds are reversible pseudosubstrate inhibitors. Four classes of carbamoyl-triazoles were synthesized and tested with respect to potency, efficacy, and selectivity. The compounds inhibiting HSL have all full efficacy, and none of the compounds were inhibitors of LPL, HL, and PL. The *N,N*-dimethyl- and piperidine-carbamoyl-triazoles was, in general, potent HSL inhibitors (nM range) but not selective due to inhibition of BChE and AChE (nM range). The morpholine carbamoyl-triazoles were weak HSL inhibitors (μ M range) and not selective as the compounds also inhibited AChE. In contrast, the *N*-methyl, *N*-phenyl carbamoyl-triazoles were selective with respect to BChE. Within this series compounds **4b** and **4g** were found to be potent HSL inhibitors with IC₅₀ values of 0.17 and 0.25 μ M, respectively, and the only compounds which did not inhibit AChE. In conclusion, two selective and potent HSL inhibitors were identified.

Further studies will be conducted to evaluate the biological importance and therapeutical significance of HSL inhibition in vitro and in vivo. On the basis of the expected importance of targeting a reduced FA mobilization from adipose tissue, HSL inhibitors might have a future for the treatment of type 2 diabetes, the metabolic syndrome, and impaired glucose tolerance.

Experimental Section

Materials and Methods. Melting points were determined on a differential scanning calorimetry instrument. NMR data were recorded on a 300 MHz and on a 400 MHz spectrometer. Assignments: Quint: quintet; sext: sextet. Elemental analyses were within 0.4% of the calculated values. Phosphatidylcholin (P-3556) and phosphatidyl-inositol (P-5954), PL (L0382), and colipase (C3028) were from Sigma. Human recombinant HSL was prepared as described by Holm et al.³⁷ Human hepatic lipase and bovine lipoprotein lipase³⁸ were kindly provided by Professor Gunilla Olivecrona, Umeå University, Sweden. Apo CII was prepared as described by Holm et al.³⁹ Different 3-phenyl or 3-alkyl-5-alkylsulfanyl-4H-[1,2,4]triazoles (**1a–p**) were prepared according to literature procedures.⁴⁰ The ¹H and ¹³C NMR data are given in the Experimental Section. Octadec-9-enoic acid 2-[12-(7-nitro-benzo[1,2,5]oxadiazol-4-ylamino)-dodecanoyloxy]-1-octadec-9-enoyloxymethyl-ethyl ester was synthesized using methods described for analogous compounds.⁴¹

General Procedure. The appropriate NH-triazole (2.26 mmol) was dissolved in DMF (2 mL) in a flame-dried reaction flask in an atmosphere of nitrogen. 1,4-Diazabicyclo[2.2.2]octane (6.77 mmol, 0.78 g) and the appropriate carbamoyl chloride (4.50 mmol) were dissolved in DMF (3 mL) in a flame-dried reaction flask under nitrogen. The dissolved NH-triazole was added, and the reaction mixture was stirred at room temperature for 16 h. The reaction mixture was evaporated to dryness, extracted with dichloromethane (3 × 30 mL) from an aqueous solution of citric acid (3%, 20 mL), dried, and evaporated to give the crude products. The crude products were recrystallized from the respective solvents given in Tables 1–3.

3-(4-Chloro-phenyl)-5-ethylsulfanyl-4H-[1,2,4]triazole, 1a. ¹H NMR 300 MHz (DMSO-*d*₆): δ 1.35 (t, *J* = 7.3 Hz, 3H), 3.18 (q, *J* = 7.3 Hz, 2H), 7.57 (d, *J* = 8.3 Hz, 2H), 7.88 (d, *J* = 8.3, 2H), 14.32 (bs, 1H). ¹³C NMR 100 MHz (DMSO-*d*₆): δ 15.01, 25.97 (bs), 127.51, 128.92, 134.15 (bs).

3-(4-Chloro-phenyl)-5-propylsulfanyl-4H-[1,2,4]triazole, 1b. ¹H NMR 300 MHz (DMSO-*d*₆): δ 0.99 (t, *J* = 7.3 Hz, 3H), 1.71 (sext, *J* = 7.2 Hz, 2H), 3.15 (t, *J* = 7.1 Hz, 2H), 7.57 (d, *J* = 8.7 Hz, 2H), 7.99 (d, *J* = 8.7 Hz, 2H), 14.31 (bs, 1H).

¹³C NMR 100 MHz (DMSO-*d*₆): δ 12.93, 22.61, 33.51, 127.52, 128.93, 134.16.

5-Methylsulfanyl-3-*p*-tolyl-1H-[1,2,4]triazole, 1c. ¹H NMR 400 MHz (DMSO-*d*₆): δ 2.36 (s, 3H, major), 2.38 (s, 3H, minor), 2.58 (s, 3H, major), 2.68 (s, 3H, minor), 7.22–7.39 (m, 2H), 7.86 (d, *J* = 7.0 Hz, 2H), 13.97 (bs, 1H, minor) 14.34 (bs, 1H, major). ¹³C NMR 100 MHz (DMSO-*d*₆): δ 13.97, 20.87, 125.79, 127.40, 128.93, 129.41, 129.73, 139.68 (bs), 141.73, 165.66.

3-Biphenyl-4-yl-5-methylsulfanyl-4H-[1,2,4]triazole, 1d. ¹H NMR 400 MHz (DMSO-*d*₆): δ 2.64 (s, 3H), 7.40 (dt, *J* = 7 Hz, 1H), 7.50 (t, *J* = 7 Hz, 2H), 7.74 (d, *J* = 7 Hz, 2H), 7.83 (d, *J* = 8.7 Hz, 2H), 8.08 (d, *J* = 8.7 Hz, 2H), 14.31 (bs, 1H). ¹³C NMR 100 MHz (DMSO-*d*₆): δ 13.81 (major), 14.37 (minor), 125.68, 126.21, 126.53, 126.66, 126.84, 127.21, 127.59, 127.94, 128.91, 128.96, 129.97, 139.00, 139.46, 140.48, 141.70, 153.18, 154.87, 160.58, 161.19.

3-Hexylsulfanyl-5-*p*-tolyl-4H-[1,2,4]triazole, 1e. ¹H NMR 400 MHz (DMSO-*d*₆): δ 0.86 (t, *J* = 6.8 Hz, 3H), 1.22–1.33 (m, 4H), 1.39 (quint, *J* = 7 Hz, 2H), 1.68 (quint, *J* = 7 Hz, 2H), 2.34 (s, 3H, minor), 2.36 (s, 3H, major), 3.10 (t, *J* = 7.2 Hz, 2H, major), 3.19 (t, *J* = 7.2 Hz, 2H, minor), 7.26 (d, *J* = 7.9 Hz, 2H, minor), 7.34 (d, *J* = 7.9 Hz, 2H, major), 7.84 (d, *J* = 7.9 Hz, 2H, major), 7.87 (d, *J* = 7.9 Hz, 2H, minor), 13.98 (bs, minor), 14.30 (bs, major). ¹³C NMR 100 MHz (DMSO-*d*₆): δ 13.80, 20.88, 21.91, 27.60, 29.18, 30.62, 31.30 (bs), 125.76, 127.40, 128.93, 129.40 (bs), 129.75, 141.72, 165.65.

3-Methylsulfanyl-5-naphthalen-2-yl-4H-[1,2,4]triazole, 1f. ¹H NMR 400 MHz (DMSO-*d*₆): δ 2.66 (s, 3H), 7.55–7.63 (m, *J* = 3 Hz, 2H), 7.92–8.01 (m, *J* = 3 Hz, 1H), 8.02–8.13 (m, 3H), 8.55 (bs, 1H), 14.38 (bs, 1H). ¹³C NMR 100 MHz (DMSO-*d*₆): δ 13.84 (major), 14.40 (minor), 123.09, 123.50, 124.13, 124.68, 125.67, 126.46, 126.98, 127.30, 127.59, 127.72, 128.18, 128.29, 128.36, 128.42, 128.74, 132.58, 132.83, 133.10, 133.45, 153.32, 155.22, 160.67, 161.50.

5-Methylsulfanyl-3-(4-trifluoromethoxy-phenyl)-1H-[1,2,4]triazole, 1g. ¹H NMR 400 MHz (DMSO-*d*₆): δ 2.66 (s, 3H), 7.51 (d, *J* = 8.6, 2H), 8.11 (d, *J* = 8.6, 2H), 14.35 (bs). ¹³C NMR 100 MHz (DMSO-*d*₆): δ 14.17, 116.24, 118.79, 121.04, 121.34, 121.41, 123.89, 127.89, 149.10.

3-(4-Methoxy-phenyl)-5-methylsulfanyl-4H-[1,2,4]triazole, 1h. ¹H NMR 400 MHz (DMSO-*d*₆): δ 2.61 (s, 3H), 3.83 (s, 3H), 7.08 (d, *J* = 8.5, 2H), 7.93 (d, *J* = 8.5, 2H), 14.17 (bs, 1H). ¹³C NMR 100 MHz (DMSO-*d*₆): δ 14.38, 55.06, 114.05, 114.67, 127.88, 129.70, 160.86.

3-Ethylsulfanyl-5-(4-methoxy-phenyl)-4H-[1,2,4]triazole, 1i. ¹H NMR 400 MHz (DMSO-*d*₆): δ 1.35 (t, *J* = 7.3, 2H), 3.15 (q, *J* = 7.3, 2H), 3.83 (s, 3H), 7.08 (d, *J* = 9.1, 2H), 7.93 (d, *J* = 9.1, 2H), 14.17 (bs, 1H). ¹³C NMR 100 MHz (DMSO-*d*₆): δ 15.07, 25.73 (bs), 55.21, 113.65, 114.27, 120.22, 127.45, 129.30, 160.45.

3-*p*-Tolyl-5-(2,2,2-trifluoro-ethylsulfanyl)-1H-[1,2,4]triazole, 1j. ¹H NMR 400 MHz (DMSO-*d*₆): δ 2.37 (s, 3H), 4.20 (q, *J* = 10.3, 2H), 7.35 (d, *J* = 8.1, 2H), 7.87 (d, *J* = 8.1, 2H), 14.52 (bs, 1H). ¹³C NMR 100 MHz (DMSO-*d*₆): δ 20.91, 32.76 (q, *J* = 32.9), 125.67 (q, *J* = 275.9), 125.97, 129.57, 140.17 (bs).

5-Methylsulfanyl-3-(4-trifluoromethyl-phenyl)-1H-[1,2,4]triazole, 1k. ¹H NMR 400 MHz (DMSO-*d*₆): δ 2.67 (s, 3H), 7.87 (d, *J* = 8.1, 2H), 8.19 (d, *J* = 8.1, 2H), 14.28 (bs, 1H). ¹³C NMR 100 MHz (DMSO-*d*₆): δ 14.15, 124.06 (q, *J* = 272.3), 125.83 (q, *J* = 3.7), 126.42, 128.37, 129.44 (q, *J* = 31.4), 164.67.

5-Methylsulfanyl-3-styryl-1H-[1,2,4]triazole, 1l. ¹H NMR 400 MHz (DMSO-*d*₆): δ 2.61 (s, 3H), 7.07 (d, *J* = 16.2, 1H), 7.32–7.46 (m, 3H), 7.49 (d, *J* = 16.2, 1H), 7.65 (dd, *J* = 7.9 and 1.6, 2H), 14.03 (bs, 1H). ¹³C NMR 100 MHz (DMSO-*d*₆): δ 13.94, 144.48 (bs), 126.97, 128.79, 134.06 (bs), 135.50.

3-(4-Chloro-phenyl)-5-(2,2,2-trifluoro-ethylsulfanyl)-1H-[1,2,4]triazole, 1m. ¹H NMR 400 MHz (CDCl₃): δ 3.91 (q, *J* = 9.4, 2H), 7.45 (d, *J* = 8.7, 2H), 7.90 (d, *J* = 8.7, 2H), 10.79 (bs, 1H). ¹³C NMR 100 MHz (DMSO-*d*₆): δ 32.90 (q, *J* = 32.90), 125.61 (q, *J* = 276.0), 127.75, 128.67, 129.14, 131.09, 134.86 (bs).

3-(4-Chloro-phenyl)-5-methylsulfanyl-1H-[1,2,4]triazole, 1n. ¹H NMR 300 MHz (DMSO-*d*₆): δ 2.66 (s, 3H), 7.35 (d, *J* = 8.7, 2H), 7.87 (d, *J* = 8.7, 2H), 11.55 (bs, 1H). ¹³C NMR

75 MHz (DMSO- d_6): δ 15.48, 127.44, 128.10, 129.48, 136.53, 158.57, 159.74.

3-(4-Chloro-phenyl)-5-hexylsulfanyl-1H-[1,2,4]triazole, 1o. ^1H NMR 300 MHz (DMSO- d_6): δ 0.85 (t, $J = 7$, 3H), 1.19–1.33 (m, 4H), 1.39 (quint, $J = 7$, 2H), 1.68 (quint, $J = 7$, 2H), 3.16 (t, $J = 7$, 2H), 7.57 (d, $J = 8.5$, 2H), 7.99 (d, $J = 8.5$, 2H), 14.31 (bs, 1H). ^{13}C NMR 75 MHz (DMSO- d_6): δ 14.18, 22.30, 27.95, 29.54, 31.00, 31.92 (bs), 127.89, 129.31, 134.60 (bs).

3-(4-Chloro-phenyl)-5-cyclopropylmethylsulfanyl-1H-[1,2,4]triazole, 1p. ^1H NMR 300 MHz (CDCl₃): δ 0.29–0.36 (m, 2H), 0.58–0.67 (m, 2H), 1.12–1.26 (m, 1H), 3.17 (d, $J = 7.5$, 2H), 7.42 (d, $J = 6.6$, 2H), 7.99 ($J = 6.6$, 2H). ^{13}C NMR 75 MHz (DMSO- d_6): δ 5.92, 11.45, 127.93 (bs), 128.30 (bs), 130, 24 (bs).

3-(4-Chloro-phenyl)-5-ethylsulfanyl-[1,2,4]triazole-1-carboxylic Acid Dimethylamide, 2a. ^1H NMR 400 MHz (CDCl₃): δ 1.39 (t, $J = 7.4$ Hz, 3H), 3.13 (bs, 6H), 3.27 (q, $J = 7.4$ Hz, 2H), 7.59 (d, $J = 8.6$ Hz, 2H), 8.03 (d, $J = 8.6$ Hz, 2H). ^{13}C NMR (CDCl₃) 100 MHz: δ 14.35, 26.49, 127.89, 128.36, 128.95, 134.65, 149.82, 158.24, 159.22. Anal. (C₁₃H₁₅ClN₄OS) C, H, N.

3-(4-Chloro-phenyl)-5-propylsulfanyl-[1,2,4]triazole-1-carboxylic Acid Dimethylamide, 2b. ^1H NMR 400 MHz (CDCl₃): δ 1.08 (t, $J = 7.5$ Hz, 3H), 1.83 (sext, $J = 7.5$ Hz, 2H), 3.23 (bs, 6H), 3.29 (t, $J = 7.5$ Hz, 2H), 7.41 (d, $J = 8.6$ Hz, 2H), 8.04 (d, $J = 8.6$ Hz, 2H). ^{13}C NMR (CDCl₃) 100 MHz: δ 13.46, 22.42, 34.73, 38.37, 127.99, 128.70, 128.81, 135.78, 150.97, 159.98, 160.12. Anal. (C₁₄H₁₇ClN₄OS) C, H, N.

5-Methylsulfanyl-3-*p*-tolyl-[1,2,4]triazole-1-carboxylic Acid Dimethylamide, 2c. ^1H NMR 400 MHz (CDCl₃): δ 2.40 (s, 3H), 2.72 (s, 3H), 3.25 (bs, 6H), 7.25 (d, $J = 8.3$ Hz, 2H), 8.00 (d, $J = 8.3$, 2H). ^{13}C NMR (CDCl₃) 100 MHz: δ 15.59, 21.49, 126.62, 127.31, 129.29, 139.97, 151.17, 160.37, 161.07. Anal. (C₁₃H₁₆N₄OS) C, H, N.

3-*p*-Tolyl-5-(2,2,2-trifluoro-ethylsulfanyl)-[1,2,4]triazole-1-carboxylic Acid Dimethylamide, 2d. ^1H NMR 400 MHz (CDCl₃): δ 2.40 (s, 3H), 3.28 (bs, 6H), 4.12 (q, $J = 9.8$ Hz, 2H), 7.25 (d, $J = 7.8$ Hz, 2H), 7.98 (d, $J = 7.8$ Hz, 2H). ^{13}C NMR (CDCl₃) 100 MHz: δ 21.50, 34.43 (q, $J = 33.7$), 39.00 (bs), 124.98 (q, $J = 27.6$), 126.67, 126.87, 129.35, 140.35, 150.76, 157.26, 161.03. Anal. (C₁₄H₁₅F₃N₄OS) C, H, N.

5-Hexylsulfanyl-3-*p*-tolyl-[1,2,4]triazole-1-carboxylic Acid Dimethylamide, 2e. ^1H NMR 400 MHz (CDCl₃): δ 0.90 (t, $J = 7.1$ Hz, 3H), 1.30–1.38 (m, 4H), 1.48 (quint, $J = 7.5$, 2H), 1.80 (quint, $J = 7.5$, 2H), 2.40 (s, 3H), 3.23 (bs, 6H), 3.31 (t, $J = 7.5$ Hz, 2H), 7.25 (d, $J = 8.1$ Hz, 2H), 7.99 (d, $J = 8.1$ Hz, 2H). ^{13}C NMR (CDCl₃) 100 MHz: δ 14.05, 21.49, 22.53, 28.49, 28.91, 31.31, 32.74, 38.85, 126.61, 127.40, 129.27, 139.91, 151.19, 159.63, 161.08. Anal. (C₁₈H₂₆N₄OS) C, H, N.

5-Methylsulfanyl-3-(4-trifluoromethoxy-phenyl)-[1,2,4]triazole-1-carboxylic Acid Dimethylamide, 2f. ^1H NMR 400 MHz (CDCl₃): δ 2.72 (s, 3H), 3.25 (bs, 6H), 7.28 (d, $J = 9.1$ Hz, 2H), 8.15 (d, $J = 9.1$ Hz, 2H). ^{13}C NMR (CDCl₃) 100 MHz: δ 15.61, 38.96 (bs), 120.45 (q, $J = 257.6$ Hz), 120.96, 128.31, 128.83, 150.36, 150.98, 159.90, 160.88. Anal. (C₁₃H₁₃F₃N₄O₂S) C, H, N.

3-(4-Methoxy-phenyl)-5-methylsulfanyl-[1,2,4]triazole-1-carboxylic Acid Dimethylamide, 2g. ^1H NMR 400 MHz (CDCl₃): δ 2.72 (s, 3H), 3.24 (bs, 6H), 3.85 (s, 3H), 6.96 (d, $J = 9.1$ Hz, 2H), 7.98 (d, $J = 9.1$, 2H). ^{13}C NMR (CDCl₃) 100 MHz: δ 15.59, 39.00 (bs), 55.34, 113.96, 122.77, 128.20, 151.20, 160.35, 160.85, 161.01. Anal. (C₁₃H₁₆N₄O₂S) C, H, N.

5-Methylsulfanyl-3-(4-trifluoromethyl-phenyl)-[1,2,4]triazole-1-carboxylic Acid Dimethylamide, 2h. ^1H NMR 300 MHz (CDCl₃): δ 2.73 (s, 3H), 3.26 (bs, 6H), 7.70 (d, $J = 8.1$, 2H), 8.23 (d, $J = 8.1$, 2H). ^{13}C NMR (CDCl₃) 100 MHz: δ 15.62, 38.95 (bs), 124.04 (q, $J = 272$), 125.57 (q, $J = 4$), 126.97, 131.57 (q, $J = 32$), 133.52, 150.88, 159.79, 161.03. Anal. (C₁₃H₁₃F₃N₄OS) C, H, N.

3-Biphenyl-4-yl-5-methylsulfanyl-[1,2,4]triazole-1-carboxylic Acid Dimethylamide, 2i. ^1H NMR 400 MHz (CDCl₃): δ 2.74 (s, 3H), 3.26 (bs, 6H), 7.37 (t, $J = 7$ Hz, 1H), 7.46 (t, $J = 7$ Hz, 2H), 7.64 (d, $J = 7$ Hz, 2H), 7.68 (d, $J = 8.2$

Hz, 2H), 8.18 (d, $J = 8.2$ Hz, 2H). ^{13}C NMR (CDCl₃) 100 MHz: δ 15.61, 38.92, 127.08, 127.13, 127.28, 127.65, 128.85, 129.03, 140.51, 142.59, 151.10, 160.57, 160.76. Anal. (C₁₈H₁₈N₄O₂S) C, H, N.

5-Methylsulfanyl-3-naphthalen-2-yl-[1,2,4]triazole-1-carboxylic Acid Dimethylamide, 2j. ^1H NMR 400 MHz (CDCl₃): δ 2.78 (s, 3H), 3.28 (bs, 6H), 7.52 (m, $J = 3$ Hz, 2H), 7.85 (m, $J = 3$ Hz, 1H), 7.90 (d, $J = 8.6$ Hz, 1H), 7.95 (m, $J = 3$ Hz, 1H), 8.18 (dd, $J = 8.6$ and $J = 1.5$ Hz, 1H), 8.64 (d, $J = 1.5$ Hz, 1H). ^{13}C NMR (CDCl₃) 100 MHz: δ 15.66, 38.87 (bs), 123.83, 126.43, 126.53, 126.78, 127.44, 127.80, 128.33, 128.63, 133.21, 134.10, 151.11, 160.67, 161.05. Anal. (C₁₆H₁₆N₄O₂S) C, H, N.

5-Methylsulfanyl-3-styryl-[1,2,4]triazole-1-carboxylic Acid Dimethylamide, 2k. ^1H NMR 400 MHz (CDCl₃): δ 2.63 (s, 3H), 3.14 (s, 3H), 3.17 (s, 3H), 7.30 (d, $J = 16.1$, 1H), 7.33–7.41 (m, 3H), 7.57 (d, $J = 7$, 2H), 7.83 (d, $J = 16.1$, 1H). ^{13}C NMR (CDCl₃) 100 MHz: δ 14.27, 37.67, 39.41, 112.26, 127.74, 128.80, 129.57, 135.37, 139.19, 150.80, 156.91, 161.81. Anal. (C₁₄H₁₆N₄O₂S) C, H, N.

[3-(4-Chloro-phenyl)-5-methylsulfanyl-[1,2,4]triazol-1-yl]-morpholin-4-yl-methanone, 3a. ^1H NMR 400 MHz (CDCl₃): δ 2.72 (s, 3H), 3.77–3.86 (m, 4H), 3.88 (bs, 4H), 7.42 (d, $J = 8.7$ Hz, 2H), 8.03 (d, $J = 8.7$ Hz, 2H). ^{13}C NMR (CDCl₃) 100 MHz: δ 15.99, 47.26 (bs), 67.03, 128.43, 128.76, 129.26, 136.43, 150.19, 160.7, 161.80. Anal. (C₁₄H₁₅ClN₄O₂S) C, H, N.

(5-Methylsulfanyl-3-*p*-tolyl-[1,2,4]triazol-1-yl)-morpholin-4-yl-methanone, 3b. ^1H NMR 400 MHz (CDCl₃): δ 2.40 (s, 3H), 2.73 (s, 3H), 3.78–3.85 (m, 4H), 3.90 (bs, 4H), 7.25 (d, $J = 8.3$ Hz, 2H), 7.98 (d, $J = 8.3$, 2H). ^{13}C NMR (CDCl₃) 100 MHz: δ 15.60, 21.51, 46.96 (bs), 66.68, 126.66, 127.06, 129.33, 140.20, 150.00, 161.02, 161.25. Anal. (C₁₅H₁₈N₄O₂S) C, H, N.

[3-(4-Chloro-phenyl)-5-hexylsulfanyl-4H-[1,2,4]triazol-1-yl]-morpholin-4-yl-methanone, 3c. ^1H NMR 400 MHz (CDCl₃): δ 0.90 (t, $J = 7.1$ Hz, 3H), 1.27–1.40 (m, 4H), 1.48 (t, $J = 7.5$ Hz, 2H), 1.81 (quint, $J = 7.5$ Hz, 2H), 3.31 (t, $J = 7.5$ Hz, 2H), 3.70–3.86 (m, 4H), 3.87 (bs, 4H), 7.41 (d, $J = 8.6$, 2H), 8.02 (d, $J = 8.6$, 2H). ^{13}C NMR (CDCl₃) 100 MHz: δ 14.04, 22.52, 28.48, 28.84, 31.29, 32.80, 46.80 (bs), 66.65, 128.03, 128.45, 128.86, 136.00, 149.83, 160.30, 160.74. Anal. (C₁₉H₂₅ClN₄O₂S) C, H, N.

[3-(4-Chloro-phenyl)-5-(2,2,2-trifluoro-ethylsulfanyl)-4H-[1,2,4]triazol-1-yl]-morpholin-4-yl-methanone, 3b. ^1H NMR 300 MHz (CDCl₃): δ 3.78–3.87 (m, 4H), 3.94 (bs, 4H), 4.12 (q, $J = 9.7$ Hz, 2H), 7.43 (d, $J = 8.5$ Hz, 2H), 8.01 (d, $J = 8.5$ Hz, 2H). ^{13}C NMR (CDCl₃) 75 MHz: δ 34.80 (q, $J = 33.7$ Hz), 47.53 (bs), 66.98, 127.07 (t, $J = 274.5$ Hz), 128.25, 128.47, 129.34, 136.78, 149.76, 158.66, 160.64. Anal. (C₁₅H₁₄ClF₃N₄O₂S) C, H, N.

[5-Ethylsulfanyl-3-(4-methoxy-phenyl)-[1,2,4]triazol-1-yl]-morpholin-4-yl-methanone, 3e. ^1H NMR 400 MHz (CDCl₃): δ 1.47 (t, $J = 7.6$ Hz, 3H), 3.32 (q, $J = 7.6$ Hz, 2H), 3.76–3.96 (m, 8H), 3.86 (s, 3H), 6.96 (d, $J = 9.1$ Hz, 2H), 8.03 (d, $J = 9.1$ Hz, 2H). ^{13}C NMR (CDCl₃) 100 MHz: δ 14.24, 27.10, 46.92 (bs), 55.35, 66.67, 113.98, 122.55, 128.24, 150.02, 160.05, 161.09, 161.11. Anal. (C₁₆H₂₀N₄O₂S) C, H, N.

[3-(4-Chloro-phenyl)-5-methylsulfanyl-[1,2,4]triazol-1-yl]-piperidin-1-yl-methanone, 3f. ^1H NMR 300 MHz (CDCl₃): δ 1.72 (bs, 6H), 2.72 (s, 3H), 3.73 (bs, 4H), 7.41 (d, $J = 8.4$ Hz, 2H), 8.40 (d, $J = 8.4$ Hz, 2H). ^{13}C NMR (CDCl₃) 100 MHz: δ 15.93, 24.68, 26.24, 48.12 (bs), 128.38, 129.06, 129.19, 136.16, 150.13, 160.44, 160.91. Anal. (C₁₅H₁₇ClN₄O₂S) C, H, N.

[3-(4-Chloro-phenyl)-5-(2,2,2-trifluoro-ethylsulfanyl)-4H-[1,2,4]triazol-1-yl]-piperidin-1-yl-methanone, 3g. ^1H NMR 400 MHz (CDCl₃): δ 1.67–1.75 (m, 6H), 3.78 (bs, 4H), 4.10 (q, $J = 9.8$ Hz, 2H), 7.42 (d, $J = 8.7$ Hz, 2H), 8.02 (d, $J = 8.7$ Hz, 2H). ^{13}C NMR (CDCl₃) 100 MHz: δ 24.60, 26.21, 34.80 (q, $J = 34.2$ Hz), 48.11 (bs), 127.12 (q, $J = 275$ Hz), 128.40, 128.57, 129.26, 136.49, 149.69, 157.89, 160.38. Anal. (C₁₆H₁₆ClF₃N₄O₂S) C, H, N.

[3-(4-Chloro-phenyl)-5-cyclopropylmethylsulfanyl-4H-[1,2,4]triazol-1-yl]-piperidin-1-yl-methanone, 3h. ^1H NMR 300 MHz (CDCl₃): δ 0.38 (q, $J = 5$ Hz, 2H), 0.64 (q, $J = 5$ Hz,

2H), 1.18–1.31 (m, 1H), 1.72 (bs, 6H), 3.26 (d, $J = 7.3$ Hz, 2H), 3.72 (bs, 4H), 7.40 (d, $J = 8.6$ Hz, 2H), 8.03 (d, $J = 8.6$ Hz, 2H). ^{13}C NMR (CDCl_3) 100 MHz: δ 5.60, 10.28, 24.31, 25.85, 38.80, 47.71 (bs), 127.98, 128.73, 128.81, 135.74, 149.75, 159.71, 160.07. Anal. ($\text{C}_{18}\text{H}_{21}\text{ClN}_4\text{OS}$) C, H, N.

[3-(4-Chloro-phenyl)-5-hexylsulfanyl-4H-[1,2,4]triazole-1-yl]-piperidin-1-yl-methanone, 3i. ^1H NMR 400 MHz (CDCl_3): δ 0.90 (t, $J = 6.8$ Hz, 3H), 1.25–1.40 (m, 4H), 1.48 (t, $J = 7.4$ Hz, 2H), 1.72 (bs, 6H), 1.80 (quint, $J = 7.4$ Hz, 2H), 3.30 (t, $J = 7.6$ Hz, 2H), 3.71 (bs, 4H), 7.41 (d, $J = 8.4$, 2H), 8.04 (d, $J = 8.4$, 2H). ^{13}C NMR (CDCl_3) 100 MHz: δ 14.04, 22.52, 24.31, 25.85, 28.46, 28.92, 31.30, 32.79, 47.84, 127.98, 128.76, 128.80, 135.73, 149.76, 159.75, 160.11. Anal. ($\text{C}_{20}\text{H}_{27}\text{ClN}_4\text{OS}$) C, H, N.

3-(4-Chloro-phenyl)-5-methylsulfanyl-[1,2,4]triazole-1-carboxylic Acid Methyl-phenyl-amide, 4a. ^1H NMR 300 MHz (CDCl_3): δ 2.70 (s, 3H), 3.53 (s, 3H), 7.15 (d, $J = 7$ Hz, 2H), 7.22–7.30 (m, 1H), 7.28 (d, $J = 8.3$ Hz, 2H), 7.35 (t, $J = 7$ Hz, 2H), 7.60 (d, $J = 8.3$ Hz, 2H). ^{13}C NMR (CDCl_3) 100 MHz: δ 15.98, 40.71, 126.45, 127.57, 128.20, 128.85, 129.03, 129.61, 136.03, 144.33, 150.51, 159.95, 160.90. Anal. ($\text{C}_{17}\text{H}_{15}\text{ClN}_4\text{OS}$) C, H, N.

3-(4-Chloro-phenyl)-5-(2,2,2-trifluoro-ethylsulfanyl)-4H-[1,2,4]triazole-1-carboxylic Acid Methyl-phenyl-amide, 4b. ^1H NMR 400 MHz (CDCl_3): δ 3.55 (s, 3H), 4.11 (q, $J = 9.6$ Hz, 2H), 7.17 (d, $J = 7$ Hz, 2H), 7.24–7.33 (m, 1H), 7.29 (d, $J = 8.3$ Hz, 2H), 7.38 (t, $J = 7$ Hz, 2H), 7.58 (d, $J = 8.3$ Hz, 2H). ^{13}C NMR (CDCl_3) 100 MHz: δ 134.48 (q, $J = 34$ Hz), 40.53, 124.88 (q, $J = 276$ Hz), 126.15, 127.49, 127.83, 127.99, 128.71, 129.34, 135.96, 143.62, 149.73, 157.25, 159.53. Anal. ($\text{C}_{18}\text{H}_{14}\text{ClF}_3\text{N}_4\text{OS}$) C, H, N.

3-(4-Chloro-phenyl)-5-cyclopropylmethylsulfanyl-4H-[1,2,4]triazole-1-carboxylic Acid Methyl-phenyl-amide, 4c. ^1H NMR 300 MHz (CDCl_3): δ 0.38 (q, $J = 5$ Hz, 2H), 0.64 (q, $J = 5$ Hz, 2H), 1.17–1.30 (m, 1H), 3.24 (d, $J = 7.4$ Hz, 2H), 3.54 (s, 3H), 7.16 (d, $J = 7$ Hz, 2H), 7.22–7.29 (m, 1H), 7.27 (d, $J = 8.5$ Hz, 2H), 7.34 (t, $J = 7$ Hz, 2H), 7.59 (d, $J = 8.5$ Hz, 2H). ^{13}C NMR (CDCl_3) 100 MHz: δ 5.99, 10.20, 38.79, 40.23, 126.02, 127.15, 127.78, 128.50, 128.61, 129.19, 135.58, 143.87, 150.11, 159.56, 159.69. Anal. ($\text{C}_{20}\text{H}_{19}\text{ClN}_4\text{OS}$) C, H, N.

3-(4-Chloro-phenyl)-5-hexylsulfanyl-4H-[1,2,4]triazole-1-carboxylic Acid Methyl-phenyl-amide, 4d. ^1H NMR 400 MHz (CDCl_3): δ 0.83 (t, $J = 7.1$ Hz, 3H), 1.21–1.32 (m, 4H), 1.40 (t, $J = 7.6$ Hz, 2H), 1.72 (quint, $J = 7.6$ Hz, 2H), 3.21 (t, $J = 7.6$ Hz, 2H), 3.46 (s, 3H), 7.08 (d, $J = 7$, 2H), 7.17 (t, $J = 7$, 2H), 7.20 (d, $J = 8.6$, 2H), 7.26 (t, $J = 7$, 2H), 7.53 (d, $J = 8.6$, 2H). ^{13}C NMR (CDCl_3) 100 MHz: δ 14.04, 22.51, 28.46, 28.83, 31.29, 32.78, 40.22, 126.00, 127.14, 127.78, 128.53, 128.61, 129.91, 135.57, 143.87, 150.13, 159.60, 159.75. Anal. ($\text{C}_{22}\text{H}_{25}\text{ClN}_4\text{OS}$) C, H, N.

5-Methylsulfanyl-3-*p*-tolyl-[1,2,4]triazole-1-carboxylic Acid Methyl-phenyl-amide, 4e. ^1H NMR 400 MHz (CDCl_3): δ 2.33 (s, 3H), 2.71 (s, 3H), 3.53 (s, 3H), 7.11 (d, $J = 8.3$ Hz, 2H), 7.16 (d, $J = 7$ Hz, 2H), 7.25 (t, $J = 7$ Hz, 1H), 7.34 (t, $J = 7$ Hz, 2H), 7.57 (d, $J = 8.3$ Hz, 2H). ^{13}C NMR (CDCl_3) 100 MHz: δ 15.57, 21.42, 40.29, 126.01, 126.45, 127.07, 127.15, 129.08, 129.18, 139.72, 144.03, 150.33, 160.08, 160.56. Anal. ($\text{C}_{18}\text{H}_{18}\text{N}_4\text{OS}$) C, H, N.

5-Hexylsulfanyl-3-*p*-tolyl-[1,2,4]triazole-1-carboxylic Acid Methyl-phenyl-amide, 4f. ^1H NMR 400 MHz (CDCl_3): δ 0.90 (t, $J = 6.9$ Hz), 1.28–1.38 (m, 4H), 1.48 (quint, $J = 7.5$ Hz, 2H), 1.80 (quint, $J = 7.5$ Hz, 2H), 2.33 (s, 3H), 3.29 (t, $J = 7.5$ Hz, 2H), 3.53 (s, 3H), 7.11 (d, $J = 8.1$ Hz, 2H), 7.16 (d, $J = 7$ Hz, 2H), 7.21–7.27 (m, 1H), 7.33 (t, $J = 7$ Hz, 2H), 7.57 (d, $J = 8.1$ Hz, 2H). ^{13}C NMR (CDCl_3) 100 MHz: δ 14.05, 21.42, 22.53, 22.70, 28.47, 28.88, 29.70, 31.31, 32.76, 40.20, 50.87, 125.97, 126.45, 127.04, 127.24, 129.06, 129.16, 139.67, 143.98, 150.36, 159.30, 160.61. Anal. ($\text{C}_{23}\text{H}_{28}\text{N}_4\text{OS}$) H, N; C: calcd, 67.62; found, 68.22.

5-Methylsulfanyl-3-(4-trifluoromethoxy-phenyl)-[1,2,4]triazole-1-carboxylic Acid Methyl-phenyl-amide, 4g. ^1H NMR 400 MHz (CDCl_3): δ 2.71 (s, 3H), 3.54 (s, 3H), 7.15 (d, $J = 8.9$, 2H), 7.17 (d, $J = 7$, 2H), 7.28 (t, $J = 7$, 1H), 7.36 (t, $J = 7$, 2H), 7.69 (d, $J = 8.9$, 2H). ^{13}C NMR (CDCl_3) 100 MHz:

δ 15.61, 40.35, 120.39 (q, $J = 257.6$ Hz), 120.75, 126.09, 127.24, 128.10, 128.66, 129.25, 143.95, 150.11, 150.19, 159.37, 160.62. Anal. ($\text{C}_{18}\text{H}_{15}\text{F}_3\text{N}_4\text{O}_2\text{S}$) C, H, N.

5-Ethylsulfanyl-3-(4-methoxy-phenyl)-[1,2,4]triazole-1-carboxylic Acid Methyl-phenyl-amide, 4h. ^1H NMR 400 MHz (CDCl_3): δ 1.46 (t, $J = 7.4$ Hz, 3H), 3.30 (q, $J = 7.4$ Hz, 2H), 3.54 (s, 3H), 3.80 (s, 3H), 6.83 (d, $J = 8.6$ Hz, 2H), 7.17 (d, $J = 7$ Hz, 2H), 7.23–7.28 (m, 1H), 7.35 (t, $J = 7$ Hz, 2H), 7.62 (d, $J = 8.4$ Hz, 2H). ^{13}C NMR (CDCl_3) 100 MHz: δ 14.25, 27.12, 40.21, 55.26, 113.75, 122.70, 125.98, 127.03, 128.02, 129.16, 144.02, 150.35, 159.05, 160.45, 160.81. Anal. ($\text{C}_{19}\text{H}_{20}\text{N}_4\text{O}_2\text{S}$) C, H, N.

Crystal Structure of 2h. Compound **2h** was crystallized from a mixture of methanol and water. The crystal structure was determined by direct methods and refined to convergence with agreement factor $R(F) = 7.00\%$ for 196 parameters against 2004 observed reflections.⁴² The molecular geometry determined is outlined in Figure 3. As can be seen, it is the N(1) isomer (Figure 2) which is formed by the carbamoylation protocol (N(2), Figure 4).

The reactive site of the inhibitor is at the C(11) atom. The geometry of this site is distorted from the expected ideal sp^2 -hybridization. This carbon, C(11), has a very short bond to N(4) of 1.330(6) Å, and a longer bond to N(2) of 1.433(6) Å. The carbonyl bond is 1.220(6) Å, which is in agreement with the range commonly observed. The bonding angles support this evidence, since O–C(11)–N(2) is small, 115.9(4)°, while O–C(11)–N(4) is wide, 123.9(5)°. The N(2)–C(11)–N(4) angle conforms to the expected value, 120.3(5)°. The remaining bond lengths and angles are in good agreement with values commonly observed in organic crystal structures.⁴³ The atoms O, C(11), N(4), C(12), and C(13) can be fitted to a plane (1) with a root-mean-square deviation (rmsd) of 0.043 Å. The triazole ring atoms fit into a plane (2) with an rmsd of 0.0014 Å, while the benzene ring atoms fit into a plane (3) with an rmsd of 0.0061 Å. The angles between plane 1 and 2 and between plane 2 and 3 are 5.5(2)° and 5.1(2)°, respectively, which makes the whole molecule close to being planar. The two torsion angles between the rings are N(1)–C(2)–C(3)–C(8) = 4.3(7)°, and N(3)–C(2)–C(3)–C(4) = 5.6(7)°. No hydrogen bonds have been located in the structure, which is not surprising, as there are no strong or medium strength hydrogen bond donors present in the molecule. The coordinates have been deposited with the CCDC.⁴⁴

Lipase Assays. The inhibition of the different lipases (HSL, HL, LPL, PL) were determined in phosphorlipid stabilized emulsion assays inspired by the HSL assay described by Mueller et al.⁴¹ and the different classical assays published for the respective enzymes. The assays were based on a new fluorochrome-labeled triacylglyceride octadec-9-enoic acid 2-[12-(7-nitro-benzol[1,2,5]oxadiazol-4-ylamino)-dodecanoyloxy]-1-octadec-9-enoyloxymethyl-ethyl ester. The transfer of the fluorochrome labeled fatty acid from the micelles to the aqueous phase induced a change in fluorescence that was monitored with an excitation wavelength of 450 nm and an emission wavelength of 545 nm. The assays were performed in black 96-well fluoroplates (DFA A/S, Copenhagen).

Maximum concentration of inhibitors for determination of IC_{50} values was 100 μM with 5-fold dilution steps in six concentrations. Each data point was determined as the average of two measurements. IC_{50} values were calculated using Prism ver. 4.0 by fitting the data to a sigmoidal dose–response (variable slope) nonlinear regression analyses.

Substrate Preparation. The fluorochrome-labeled triacylglyceride (5 mg/mL in chloroform, 135 μl) and a solution of phosphorlipids (phosphatidylcholin and phosphatidylinositol 3:1 in chloroform) (20 mg/mL, 8 μl) were flushed with nitrogen for 10 min. KPI-buffer (100 mM potassium phosphate-HCl, pH 7.0, 2 mL) was added and the mixture sonicated for 2×1 min, further KPI-buffer (1 mL) was added and sonicated for 4×30 s. BSA (20% (w/v) in KPI-buffer, 1 mL) was added and mixed carefully by inversion. PED-BSA buffer (20 mM potassium

phosphate-HCl, pH 7.0; 1 mM EDTA; 1 mM dithioerythritol (DTE); 0.02% (w/v) fatty acid free BSA) (8 mL) was added and mixed.

This substrate solution (6.6 $\mu\text{g/mL}$) was used for all lipase assays except for PL. For PL the PED-BSA buffer was substituted with the following TRIS buffer (10 mM TRIS-HCl, pH 8.0; 8 mM taurodeoxycholic acid sodium salt (NaTDC); 0.3 M sodium chloride; 2 mM calcium chloride).

Hormone Sensitive Lipase Assay. A 12 $\mu\text{g/mL}$ portion of HSL (10 μL) was mixed with the respective inhibitor (20 μL) in PED-BSA buffer (pH 7.0, 70 μL) directly in the fluoroplates and preincubated for 30 min at 25 °C while shaking. Before addition of 5 mM substrate solution (100 μL), the basal fluorescence level was measured at $t = 0$ min and the fluorescence level was measured again at $t = 120$ min.

Hepatic Lipase Assay. A 1 $\mu\text{g/mL}$ mixture of HL (50 μL) and the inhibitor (2.5 μL) both diluted in DOC buffer (10 mM TRIS-HCl, pH 8.5, and 5 mM sodium deoxycholate) was preincubated in Micronic tubes for 70 min at 25 °C while shaking. Sodium chloride (5 M, (45 μL), 0.1 M TRIS-HCl (pH 8.5, 45 μL), and the preincubation mixture (10 μL) were added to the fluoroplates. The fluorescence level was measured at $t = 0$ min before addition of the lipase substrate (6.6 $\mu\text{g/mL}$, 100 μL). The fluoroplates were then incubated at 37 °C while shaking and the level of fluorescence was measured at $t = 120$ min.

Lipoprotein Lipase Assay. A 1 $\mu\text{g/mL}$ mixture of LPL (400 μL) and the inhibitor (2.0 μL) both diluted with DOC buffer were preincubated in Micronic tubes for 60 min at 25 °C while shaking. A TRIS buffer (0.3 M TRIS-HCl; 0.2 M sodium chloride; 0.2 mg/mL heparin, and 120 mg/mL BSA, pH 8.5) (90 μL), rat or human APO CII (5 μL), and the preincubation mixture (5 μL) and substrate (100 μL) were mixed in the fluoroplates and incubated at 37 °C. The fluorescence level at $t = 0$ min and the level of fluorescence at $t = 120$ min were measured.

Pancreatic Lipase Assay. A mixture of PL (1 $\mu\text{g/mL}$) and colipase (5 $\mu\text{g/mL}$) (95 μL) and inhibitor (5 μL) was preincubated for 40 min at 25 °C with shaking in Micronic tubes. A TRIS buffer (0.15 M sodium chloride; 10 mM TRIS-HCl, pH 8.0; and 1 mM NaTDC) (90 μL), the preincubation mixture (10 μL), and substrate (100 μL) were mixed in the fluoroplates and incubated at 37 °C. The fluorescence levels at $t = 0$ min and at $t = 60$ min were measured.

Esterase Assays. The AChE substrate acetylthiocholin and BChE substrate butyrylthiocholin were cleaved by the respective enzyme to give thiocholin and acetate or butyrate. By addition of DTNB (dithiobisnitrobenzoic acid, Ellmans reagent) a yellow color was developed, which was proportional to the product formed and hence with the enzyme activity. The color intensity was measured at 405 nm on a spectrophotometer. Results are given as percent activity relative to an uninhibited sample (no compound). Dilutions of inhibitors as well as curve fitting of data and IC₅₀ estimations were done as described for the lipase assays.

AChE and BChE Assays. The method of Ellman⁴⁵ was applied. A solution of the inhibitor (50 μL) was added to a 100 U/mL solution of AChE/BChE (50 μL) and preincubated for 30 min at 25 °C. A phosphate buffer (0.1 M potassium phosphate-HCl, pH 8.0) (100 μL), 0.075 M acetylthiocholin or butyrylthiocholin (10 μL), and 0.01 M DTNB in aqueous sodium hydrogen carbonate (1 mg/mL, 10 μL) were mixed with the preincubation mixture (10 μL) in microtiterplates. The absorption at 405 nm was measured at a spectrophotometer at $t = 0$ and after incubation for 15 min at 37 °C with shaking.

Acknowledgment. Anette Frost Jensen, Novo Nordisk A/S, and Inger Søtofte, Technical University of Denmark, are gratefully acknowledged for collection of X-ray diffraction data and data processing for **2h**. Dr. Christian Fledelius and Professor Hans Evert Thornqvist are gratefully acknowledged for fruitful discussions and comments. The technical assistance from

Freddy Z. Pedersen and Flemming Gundertofte is highly appreciated.

Supporting Information Available: Crystal data and structure refinement, bond lengths, bond angles, and torsion angles of interest for **2h**. This material is available free of charge via the Internet at <http://pubs.acs.org>.

References

- Ginsberg, H.; Plutzky, J.; Sobel, E. Review of metabolic and cardiovascular effects of oral antidiabetic agents: beyond glucose-lowering. *J. Cardiovasc. Risk* **1999**, *6*, 337–346.
- Zavaroni, I.; Bonini, L.; Gasparini, P.; Barilli, A. L.; Zuccarelli, A.; Dall'Aglio, E.; Delsignore, R.; Reaven, G. M. Hyperinsulinemia in a normal population as a predictor of noninsulin-dependent diabetes mellitus, hypertension, and coronary heart disease: the Barilla factory revisited. *Metabolism* **1999**, *48*, 989–994.
- Cobb, J.; Dukes, I. Recent advances in the Development of Agents for Treatment of Type 2 Diabetes. *Annu. Rep. Med. Chem.* **1998**, *33*, 213–221.
- Bailey, C. J. Potential new treatments for type 2 diabetes. *TIPS* **2000**, *21*, 259–265.
- Frayn, K. N. Adipose tissue as a buffer for daily lipid flux. *Diabetologia* **2002**, *45*, 1201–1210.
- Unger, R. H. Lipotoxicity in the pathogenesis of obesity-dependent NIDDM. Genetic and clinical implications. *Diabetes* **1995**, *44*, 863–870.
- Boden, G. Role of fatty acids in the pathogenesis of insulin resistance and NIDDM. *Diabetes* **1997**, *46*, 3–10.
- Bergman, R. N.; Ader, M. Free Fatty Acids and Pathogenesis of Type 2 Diabetes Mellitus. *Trends Endocrinol. Metab.* **2000**, *11*, 351–356.
- Kim, J. K.; Fillmore, J. J.; Chen, Y.; Yu, C.; Moore, I. K.; Pypaert, M.; Lutz, E. P.; Kako, Y.; Velez-Carrasco, W.; Goldberg, I. J.; Breslow, J.; Schulman, G. I. Tissue-specific overexpression of lipoprotein lipase causes tissue-specific insulin resistance. *PNAS* **2001**, *98*, 7522–7527.
- Groop, L. C.; Saloranta, C.; Shank, M.; Bonadonna, R. C.; Ferrannini, E.; DeFronzo, R. A. The role of free fatty acid metabolism in the pathogenesis of insulin resistance in obesity and noninsulin-dependent diabetes mellitus. *J. Clin. Endocrinol. Metab.* **1991**, *72*, 96–107.
- Large, V.; Arner, P. Regulation of lipolysis in humans. Pathophysiological modulation in obesity, diabetes and hyperlipidemia. *Diabetes Metab.* **1998**, *24*, 409–418.
- Coppack, S. W.; Evans, R. D.; Fisher, R. M.; Frayn, K. N.; Gibbons, G. F.; Humphreys, S. M.; Kirk, M. L.; Potts, J. L.; Hockaday, T. D. Adipose tissue metabolism in obesity: lipase action in vivo before and after a mixed meal. *Metabolism* **1992**, *41*, 264–272.
- Sztalryd, C.; Komaromy, M. C.; Kraemer, F. B. Overexpression of Hormone-sensitive Lipase prevents Triglyceride accumulation in Adipocytes. *J. Clin. Invest.* **1995**, *95*, 2652–2661.
- Kraemer, F. B.; Shen, W.-J. Hormone sensitive lipase: Control of intracellular tri-(di)-acylglycerol and cholesteryl ester hydrolyses. *J. Lipid Res.* **2002**, *43*, 1585–1594.
- Langin, D.; Holm, C.; Lafontan, M. Adipocyte hormone sensitive lipase: a major regulator of lipid metabolism. *Proc. Nutr. Soc.* **1996**, *55*, 93–109.
- Sztalryd, C.; Kraemer, F. B. Regulation of Hormone-Sensitive Lipase in Streptozotocine-Induced Diabetic Rats. *Metab., Clin. Exp.* **1995**, *44*, 1391–1396.
- Lafontan, M.; Langin, D. Neuro-humoral regulation of lipolysis: Physiological and pathological aspects. *Medicine/Sciences* **1998**, *14*, 865–876.
- Petry, S.; Schoenafinger, K.; Mueller, G.; Baringhaus, K.-H. Substituted 3-phenyl-5-alkoxy-1,3,4-oxadiazol-2-ones and their use as lipase inhibitors. *PCT Appl.* WO 0117981, 2001.
- Schoenafinger, K.; Petry, S.; Mueller, G.; Baringhaus, K.-H. Substituted 3-phenyl-5-alkoxy-1,3,4-oxadiazol-2-ones and their use thereof for inhibiting hormone-sensitive lipase. *PCT Appl.* WO 0166531, 2001.
- Claus, T. H.; Lowe, D. B.; Yang, L.; Burns, M.; Daly, M.; Keiper, C.; Qi, N.; Salhanick, A.; Magnuson, S.; Clairmont, K. B. An inhibitor of hormone sensitive lipase (HSL) reduces plasma FFA and glycerol levels and prevent CL316, 243- induced insulin secretion. *Diabetes* **2002**, *51*, (suppl 2) A335.
- Contreras, J. A.; Marie Karlsson, M.; Østerlund, T.; Laurell, H.; Svensson, A.; Holm, C. Hormone-sensitive Lipase Is Structurally Related to Acetylcholinesterase, Bile Salt-stimulated Lipase, and Several Fungal Lipases. *J. Biol. Chem.* **1996**, *271*, 31426–31430.
- Fredrikson, G.; Strålfors, P.; Nilsson, N. O.; Belfrage, P. Hormone-sensitive lipase of rat adipose tissue. Purification and some properties. *J. Biol. Chem.* **1981**, *256*, 6311–6320.

- (23) Cook, K. G.; Yeaman, S. J.; Strålfors, P.; Fredrikson, G.; Belfrage, P. Direct evidence that cholesterol ester hydrolase from adrenal cortex is the same enzyme as hormone-sensitive lipase from adipose tissue. *Eur. J. Biochem.* **1982**, *125*, 245–249.
- (24) Lee, F. T.; Adams, J. B.; Garton, A. J.; Yeaman, S. J. Hormone-sensitive lipase is involved in the hydrolysis of lipoidal derivatives of estrogens and other steroid hormones. *Biochim. Biophys. Acta* **1988**, *963*, 258–264.
- (25) Wei, S.; Lai, K.; Patel, S.; Piantedosi, R.; Shen, H.; Colantuoni, V.; Kraemer, F. B.; Blaner, W. S. Retinyl ester hydrolysis and retinol efflux from BFC-1beta adipocytes. *J. Biol. Chem.* **1997**, *272*, 14159–14165.
- (26) Liu, T.-X.; Sparks, A. N., Jr.; Yue, B. Toxicity and Efficacy of Triazamate Against Turnip Aphid (Homoptera: Aphididae) on cabbage. *J. Entomol. Sci.* **2001**, *3*, 244–250.
- (27) Wei, Y.; Contreras, J. A.; Sheffield, P.; Osterlund, T.; Derewenda, U.; Kneusel, R. E.; Matern, U.; Holm, C.; Derewenda, Z. S. Crystal structure of brefeldin A esterase, a bacterial homologue of the mammalian hormone-sensitive lipase. *Nat. Struct. Biol.* **1999**, *6*, 340–345.
- (28) Simone, D. G.; Stefania, G.; Manco, G.; Lang, D.; Rossi, M.; Pedone, C. A Snapshot of a Transition State Analogue of A Novel Thermophilic Esterase Belonging to the Subfamily of Mammalian Hormone-sensitive Lipase. *J. Mol. Biol.* **2001**, *303*, 761–771.
- (29) Sanchez, R.; Sali, A. Comparative protein structure modelling. Introduction and practical examples with modeller. *Methods Mol. Biol.* **2000**, *143*, 97–129.
- (30) Østerlund, T.; Contreras, J. A.; Holm, C. Identification of essential aspartic acid and histidine residues of hormone-sensitive lipase: apparent residues of the catalytic triade. *FEBS Lett.* **1997**, *403*, 259–262.
- (31) Feaster, S. R.; Lee, K.; Baker, N.; Hui, D. Y.; Quin, D. M. Molecular Recognition by Cholesterol Esterase of Active Site Ligands: Structure–Reactivity Effects for inhibition by Aryl Carbamates and Subsequent Carbamylenzyme Turnover. *Biochemistry* **1996**, *35*, 16723–16734.
- (32) McLeish, M. J.; Kenyon, G. L. Approaches to the Rational Design of Enzyme Inhibitors, Rational Design of Covalently Binding Enzyme Inhibitors. *Burger's Medicinal Chemistry and drug Discovery*; John Wiley and Sons, Inc.: New York, 2003; pp 19–22.
- (33) Rampa, A.; Bisi, A.; Valenti, P.; Recanatini, M.; Cavalli, A.; Andrisano, V.; Cavrini, V.; Fin, L.; Buriani, A.; Giusti, P. Acetylcholinesterase Inhibitors: Synthesis and Structure–Activity Relationship of ω -[N-Methyl-N-(3-alkylcarbamoyloxyphenyl)-methyl]aminoalkoxyheteroaryl Derivatives. *J. Med. Chem.* **1998**, *41*, 3976–2986.
- (34) Huang, J.; Bushey, D. F. Novel 1,2,3-Oxadiazol-2(3H)-ones as Potential Pest Control Agents. *J. Agric. Food Chem.* **1987**, *35*, 368–373.
- (35) Perola, E.; Cellai, L.; Lamba, D.; Filocamo, L.; Brufani, M. Long chain analogues of physostigmine as potential drugs for Alzheimer's disease: new insights into the mechanism of action in the inhibition of acetylcholinesterase. *Biochim. Biophys. Acta*, **1997**, *1343*, 41–50.
- (36) Rampa, A.; Piazzzi, L.; Belluti, F.; Gobbi, S.; Bisi, A.; Bartolini, M.; Andrisano, V.; Cavrini, A.; Cavalli, A.; Recanatini, M.; Valenti, P. Acetylcholinesterase Inhibitors: SAR and Kinetic Studies on ω -[N-Methyl-N-(3-alkylcarbamoyloxyphenyl)-methyl]-aminoalkoxyaryl Derivatives. *J. Med. Chem.* **2001**, *44*, 3810–3820.
- (37) Contreras, J. A.; Danielsson, B.; Johansson, C.; Osterlund, T.; Langin, D.; Holm, C. Human hormone sensitive lipase—expression and large-scale purification from a baculovirus/insect cell system. *Protein Expression Purif.* **1998**, *12*, 93–99.
- (38) Bengtson-Olivecrona, G.; Olivecrona, T. Phospholipase activity of milk lipoprotein lipase. *Methods Enzymol.* **1991**, *197*, 345–356.
- (39) Holm, C.; Olivecrona, G.; Ottoson, M. Assays of lipolytic enzymes. *Methods Mol. Biol.* **2001**, *155*, 97–119.
- (40) Sato, M.; Fukada, N.; Kurauchi, M.; Takeshima, T. *Synthesis* **1981**, *7*, 554–557.
- (41) Mueller, G.; Petry, S.; Jordan, H.; Kleine, H.; Wenzel, H.; Determination of complex phosphorlipid/lipid structures using synthetic fluorescence-marked acylglycerides. PTC Appl. WO 00/67025, 2000.
- (42) Bruker AXS. SHELXTL v. 5.10. Software for single-crystal structure determination. Bruker AXS, Inc.: Madison, WI. 1997.
- (43) Allen, F. H.; Kennard, O.; Watson, D. G.; Brammer, L.; Orpen, A. G.; Taylor, R. *J. Chem. Soc., Perkin Trans. 2* **1987**, 1–21.
- (44) Crystallographic data for the structure has been deposited with the Cambridge Crystallographic Data Centre as Supplementary Publication No. CCDC 223674. Copies of the data can be obtained free of charge on application to CCDC 12 Union Road, Cambridge CB2 1EZ, U.K., or on e-mail: deposit@ccdc.ac.uk.
- (45) Ellman, G. L.; Courtney, K. D.; Andres, V., Jr.; Featherstone, R. M. A new and rapid determination of acetylcholinesterase activity. *Biochem. Pharmacol.* **1961**, *7*, 88–95.

JM031004S